ICNTC-2020 Special Issue

J. Indian Chem. Soc.,
Vol. 97, No. 10c, October 2020, pp. 2055-2061

Preparation and CO_2 permeabilities of PEBA mixed matrix membranes with metal organic frameworks

Nagehan Çelik and Sennur Deniz*

[a]Department of Chemical Engineering, Yildiz Technical University, Davutpasa, Istanbul, Turkey

E-mail: sennurdeniz@gmail.com

Manuscript received online 20 October 2020, revised and accepted 31 October 2020

Carbon dioxide separation is an important area in industrial gas separation systems such as adsorption, absorption and membrane gas separation processes to cut back or rule out CO_2 emission to decrease its negative impact on climate change and polymeric membranes take a great deal of attention in gas separation. The most important polymers used in industrial membrane gas separation are cellulose acetate, polyimide, polysulfone, ethylene oxide/propylene oxide-amide copolymers. In this study, poly(ether-*b*-amide) (PEBA) was selected as a membrane matrix to prepare the polymer nanocomposite membranes containing with MOF particles. PEBA copolymers are thermoplastic elastomers and show high permeability and good separation factors. Cu-MOF nanocrystals was synthesized by the solvo-thermal method using with two different synthesis methods and two different modulators (acetic acid or trimethylamine). Copper-based metal organic framework (Cu-MOF) nanocrystals were added to the PEBA membrane matrix to increase the separation performance depending on the selectivity and permeability parameters. PEBA/Cu-MOF membranes were fabricated by the loading of Cu-MOF 10 wt% in PEBA matrix. The effects of Cu-MOF loadings and structures were investigated on the morphologies and CO_2 gas permeabilities of PEBA MMMs. To compare with pure PEBA membrane, CO_2 permeabilities of PEBA/Cu-MOF membranes were measured at 35°C and 3 bar feed pressure.

Keywords: Mixed-matrix membranes, PEBA, Cu-MOF, gas separation, permeability.

Introduction

Gas mixtures are separated in industrial systems by the using of cryogenic distillation, adsorption and polymeric membranes. Membrane technologies take a great deal of attention in gas separation, because membrane-based systems have advantages such as low energy consumption, low cost, easy installation and small footprint[1]. Membrane systems can be used in many fields such as natural gas carbon dioxide removal, flue gas carbon dioxide capture, biogas upgrading[2]. Carbon dioxide separation is an important area in industrial gas separation systems to reduce or eliminate CO_2 emission to decrease its negative impact on climate change. The most important parameters emphasized when examining the efficiency of membrane systems are selectivity and permeability. These parameters of membrane material affect the economy of a gas separation membrane process. Permeability is the rate at which any compound penetrates through a membrane, it depends on thermodynamic and kinetic factors. Selectivity is the ability of a membrane to perform a distinction[3]. Polymeric membranes are of great interest in membrane gas separation systems. Unfortunately, an important and restrictive condition in the development of these membranes for gas separation applications is the trade-off between permeability and selectivity, first demonstrated by Robeson[4].

Mixed-matrix membrane with inorganic filler particles introducing in polymer matrix could associated the advantages of high-performance from inorganic membranes and easy production from polymeric membranes, which is thus a kind of emerging membrane for CO_2 removing in the past two decades[5]. Fillers which are included polymer matrix can be different types such as zeolites, carbon molecular sieves, silicas, metal oxides, carbon nanotubes, metal organic frameworks[6]. Fig. 1 shows schematic illustration of gas separation process using MMMs[7].

Metal-organic framework (MOF) is a material class of

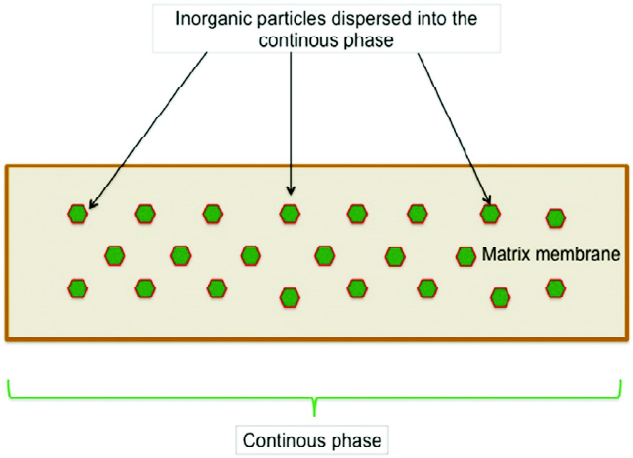

Fig. 1. Schematic illustration of gas separation process using MMMs.

nano-sized porous structures consisting of metal ions or clusters and organic linkers, exhibiting the singular properties of organic and inorganic parts (Fig. 2). The most important advantages of MOFs are huge surface areas and tunable pore size and they can also facilitate stronger interactions with the polymeric matrix and reduce the interfacial microvoids[8].

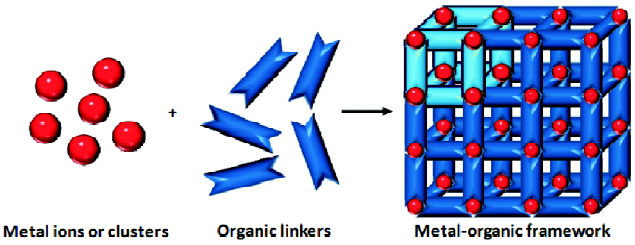

Fig. 2. Schematic illustration for the preparation of a metal organic framework[9].

In this work, crystals of Cu-MOF were synthesized to obtain an optimal interface in the mixed-matrix membrane material. Poly(ether-*b*-amide) (PEBA) was chosen as polymer material. PEBA copolymers are thermoplastic elastomers and Fig. 3 shows chemical structure of PEBA. These copolymers are used for carbon dioxide separation and show high

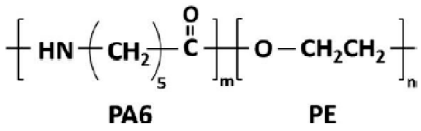

Fig. 3. Chemical structure of PEBA.

permeability and good separation factors because of large solubility coefficients of carbon dioxide due to poly ether oxide component of the material[10].

Experimental

Materials:

Copper(II) acetate monohydrate (98%, Acros Organics), copper(II) nitrate trihydrate (99%, Acros Organics), 1,3,5-benzene tricarboxylic acid (98%, Acros Organics), *N,N*-dimethylformamide (Riedel-de Haen), ethanol (J. T. Baker), dichloromethane (99.8%, Fisher), acetic acid (J. T. Baker) and triethylamine (99%, Acros Organics) were used.

Cu-MOF synthesis:

Cu-MOF nanocrystals were synthesized by two different solvothermal synthesis methods. The first synthesis procedure of Cu-MOF crystals (These crystals are symbolized Cu-MOF1) was sustained based on Brinda *et al*. report[11]. 1.612 g $Cu(AC)_2.H_2O$ was dissolved in 8 mL deionized water/8 mL EtOH/8 mL DMF and mixed with a solution containing 1 g 1,3,5-benzentricarboxylic acid in 8 mL deionized water/8 mL EtOH/8 mL DMF and triethylamine (TEA) is added as a modulator. The final solution was stirred at room temperature for 23 h. After that, the Cu-MOF1 crystals were centrifuged and washed with DMF and DCM.

The second synthesis procedure of Cu-MOF crystals, symbolized as Cu-MOF2, was sustained based on Nobar report[12]. 1.240 g $Cu(NO_3)_2.3H_2O$ was dissolved in 16.98 mL deionized water and mixed with a solution containing 0.59 g 1,3,5-benzentricarboxylic acid in 16.87 mL EtOH. Two of the same mixtures were prepared. One of the mixtures contained triethylamine as a modulator (Cu-MOF2T) and the other of the mixtures contained acetic acid as a modulator (Cu-MOF2A). Final solutions were stirred at 100°C for 24 h. After that, Cu-MOF2A and Cu-MOF2T crystals synthesized by using this procedure were centrifuged and washed with deionized water and ethanol.

Preparation of PEBA/Cu-MOF mixed matrix membranes:

In order to prepare MMMs, PEBA and ethanol/deionized water (70:30) are mixed for 24 h and after that the solution is refluxed for 4 h at 80°C and the 3 wt% polymer solution was obtained.

Cu-MOF1 and Cu-MOF2 nanoparticles were added (10 wt%) and dispersed in PEBA polymer solution and stirred at

room temperature for 24 h. After the stirring, PEBA/Cu-MOF1 solution was transferred to petri dishes by solution-casting method and waiting for 24 h at room temperature. After that, it was subjected to heat treatment at 35°C for 24 h, 50°C for 24 h, 50°C for 24 h (under the vacuum) and 70°C (under the vacuum) for 3 h respectively. PEBA/Cu-MOF2A and PEBA/Cu-MOF2T solutions were transferred to petri dishes by solution-casting method and waiting for 48 h at room temperature. After that, it was subjected to heat treatment at 35°C for 48 h, 50°C for 24 h, 50°C for 24 h (under the vacuum) and 70°C (under the vacuum) for 3 h, respectively. The PEBA/Cu-MOF1 and PEBA/Cu-MOF2 MMMs were masked with aluminum tape and kept in desiccator until the gas permeability measurements.

Characterizations:

Crystal structure of the Cu-MOF1 nanocrystals were characterized by X-ray diffraction (XRD). Surface of Cu-MOF1 nanocrystals were analyzed by SEM (scanning electron microscope). The chemical groups Cu-MOF1 nanocrystals were analyzed by Fourier transform infrared (FTIR). Adsorption-desorption of N_2 in the Cu-MOF1 nanocrystals were measured. BET surface area of Cu-MOF1 was obtained from the N_2 adsorption-desorption isotherms.

Crystal structure of the PEBA/Cu-MOF1 MMM was investigated by X-ray diffraction (XRD). Morphology of PEBA/Cu-MOF1 MMM was analyzed by SEM (scanning electron microscope). The chemical groups PEBA/Cu-MOF1 MMM was analyzed by Fourier transform infrared (FTIR).

Gas permeation measurements:

Pure gas permeations of all membranes were measured using constant-volume system at 35°C and 3 bar constant feed pressure. The membrane and the permeation system were kept under vacuum overnight before test for each gas, then the measurement tests were started.

The gas transport mechanism in gas separation membranes proceeds according to the solution-diffusion model[13]. The permeability and selectivity values of each gas are calculated with the data obtained at the end of the experiment.

Results and discussion

Characterization of Cu-MOF1:

SEM images of Cu-MOF crystals are shown in Fig. 4 and SEM images show that synthesized Cu-MOF nanocrystals

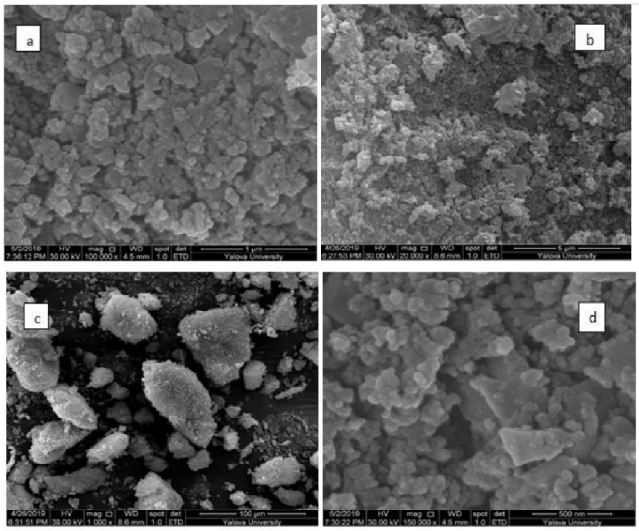

Fig. 4. SEM images of Cu-MOF1 nanocrystals.

are agglomerated.

FTIR spectra of Cu-MOF1 crystals are shown in Fig. 5. The FTIR spectra shows absorption in the wave numbers range of 500–700, 1400–1450, 1700–1800 cm^{-1}. Cu-O bond may be reason of the absorption band between 500–700 cm^{-1} and aromatic ring may be reason of the adsorption band between 1400–1450 cm^{-1}.

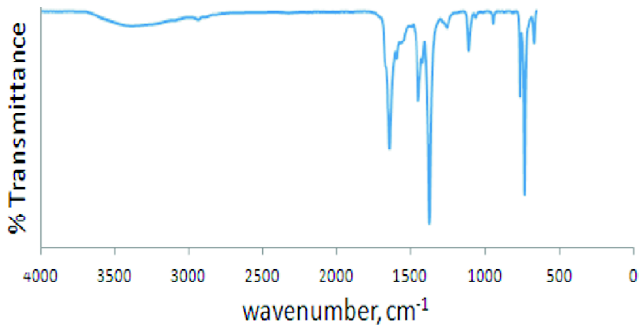

Fig. 5. FTIR spectrum of Cu-MOF1.

The structure of the Cu-MOF1 was characterized by XRD (Fig. 6). The X-ray diffractogram shows intense peaks in the 2θ range of 10–20 and these are characteristic peaks of Cu-MOF1 nanocrystals[11].

N_2 isotherm of Cu-MOF1 crystals are shown in Fig. 7. The Cu-MOF1 crystals have high adsorption capacity. The N_2 isotherms adapt type-II isotherm that means adsorption takes place in multiple layers[14].

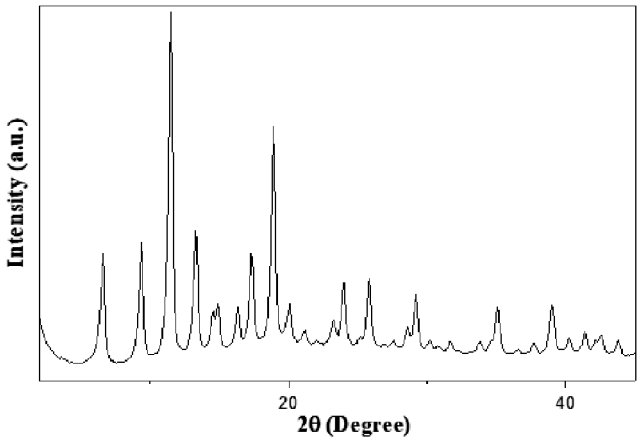

Fig. 6. XRD pattern of Cu-MOF1.

BET analysis of the Cu-MOF1 nanocrystals are shown in Table 1 and the BET surface area is 1322.96 m^2/g and these crystals have high surface area.

Table 1. BET analyses of Cu-MOF1

MOF type	BET surface area (m^2/g)	Pore volume (cm^3/g)	Average pore diameter (nm)
Cu-MOF1	1322.96	0.4176	3.1660

Characterization of PEBA/Cu-MOF1 MMMs:

SEM images of PEBA/Cu-MOF1 MMMs are shown in Fig. 8 and it can be seen that there is not an uniform distribution in polymer matrix due to the agglomeration of Cu-MOF nanocrystals.

XRD patterns of PEBA/Cu-MOF1 MMMs are shown in Fig. 9 and the X-ray diffractogram shows intense peaks in the 2θ range of 10–26. The sharp peak around 2θ degree of 24° stands for the crystalline region (PA segment) of PEBA, other peaks in different positions relate to the remaining amorphous region[15].

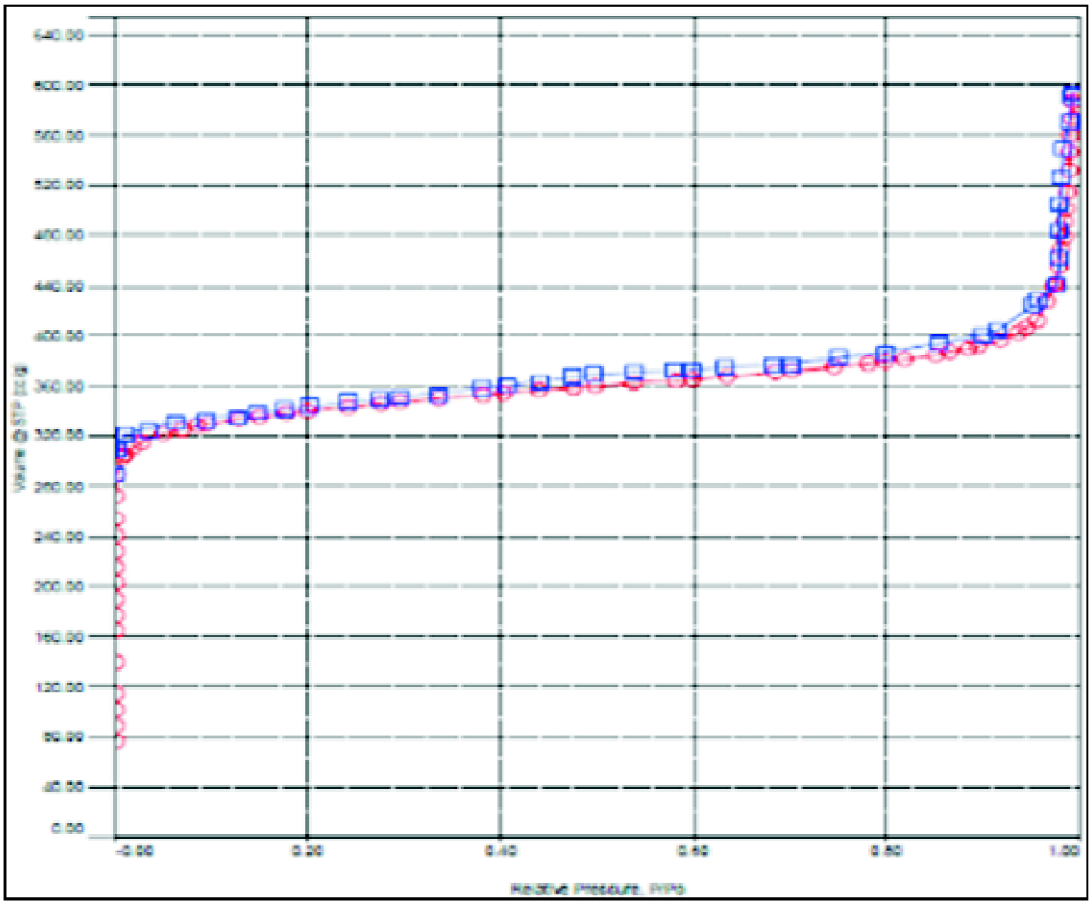

Fig. 7. N_2 isotherms of Cu-MOF1.

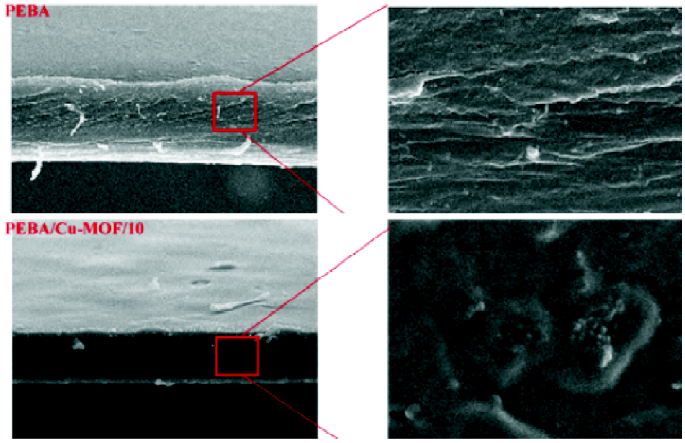

Fig. 8. SEM images of (a) PEBA membranes and (b) PEBA/Cu-MOF1-10 MMMs.

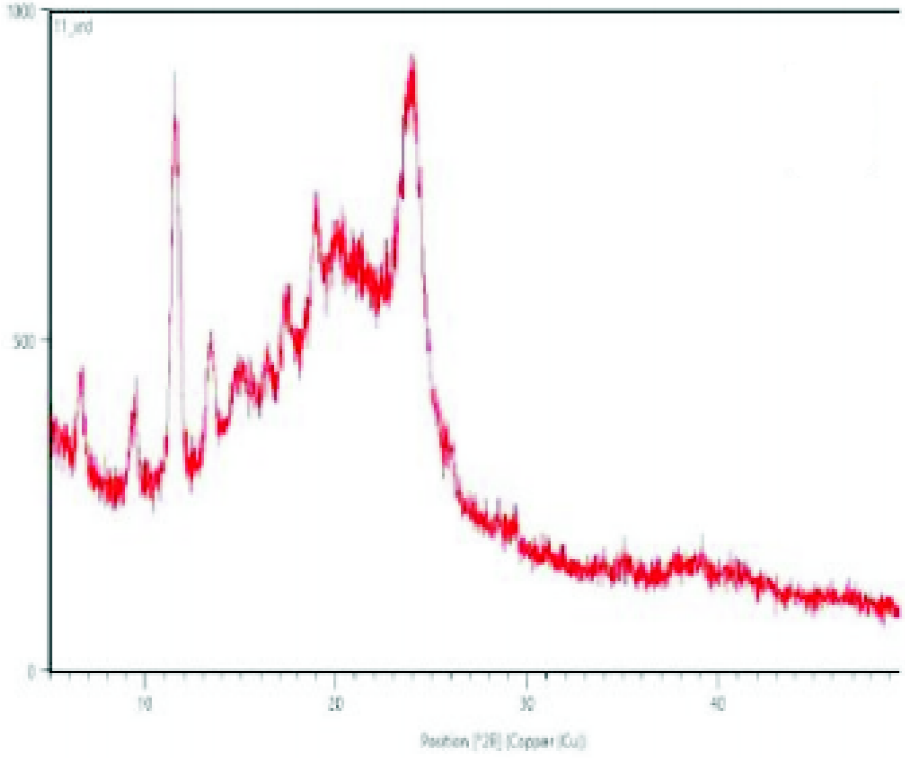

Fig. 9. XRD patterns of PEBA/Cu-MOF1 MMMs

FTIR spectra of PEBA/Cu-MOF1 MMMs are shown in Fig. 10 and it is seen that characteristic peaks specific to the molecular structure of PEBA are compatible with the literature[12].

Gas separation performance:

Before measuring the permeabilities of the MMMs, the measuring of gas permeability of the neat PEBA membrane was studied at 3 bar constant feed pressure and 35°C. Then, gas permeabilities of all MMMs were measured for N_2, CH_4 and CO_2 pure gases and calculated the ideal selectivity (α) values of CO_2/N_2 and CO_2/CH_4. Pure gas permeability values of MMMs are shown in Table 1 and pure gas selectivitiy

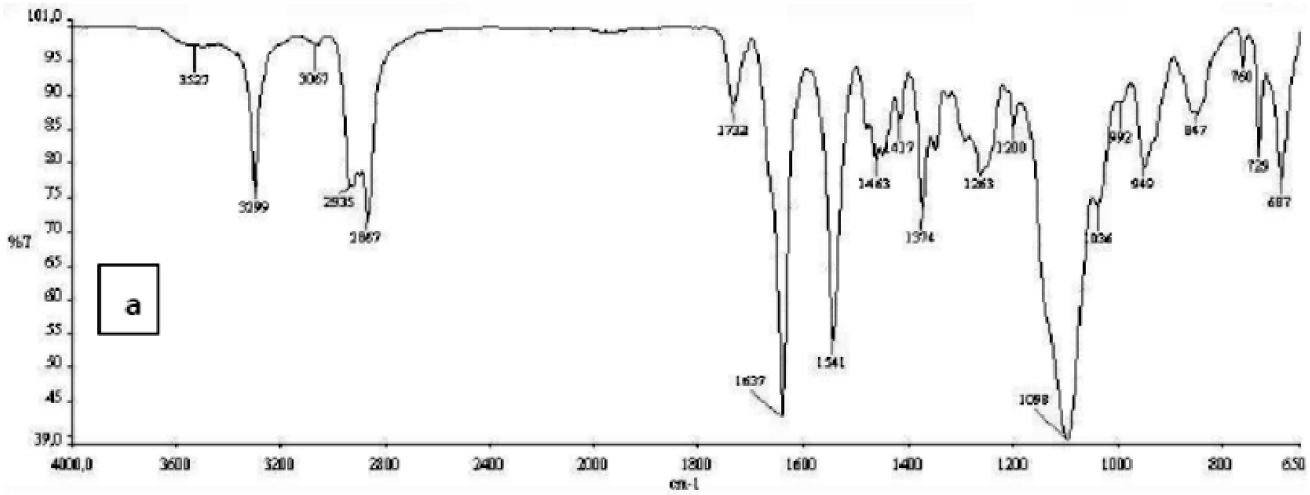

Fig. 10. FTIR spectrum of PEBA/Cu-MOF1 MMMs.

Table 2. Gas permeability values of PEBA/Cu-MOFs MMMs

Membrane	Permeability, P (Barrer*)		
	N_2	CH_4	CO_2
PEBA	0.55	2.50	30.66
PEBA/Cu-MOF1-10	5.55	2.93	28.40
PEBA/Cu-MOF2A-10	1.19	2.52	42.58
PEBA/Cu-MOF2T-10	0.98	3.17	50.77

*1 Barrer = 10^{-10} $\frac{cm^3_{STP}.cm}{cm^2.s.cm.Hg}$

Table 3. Selectivitiy values of PEBA/Cu-MOFs MMMs

Membrane	Ideal selectivity, α	
	α_{CO_2/N_2}	α_{CO_2/CH_4}
PEBA	55.74	12.26
PEBA/Cu-MOF1-10	5.11	9.60
PEBA/Cu-MOF2A-10	35.78	16.89
PEBA/Cu-MOF2T-10	51.80	16.01

values of MMMs are shown in Table 2.

The comparison of the permeability and selectivity values with the Robeson plot is as in Fig. 11.

According to Fig. 11, PEBA/Cu-MOF2T-10 MMMs can be used for gas separation and they are in a very good condition according to the case studies in the literature[16,17].

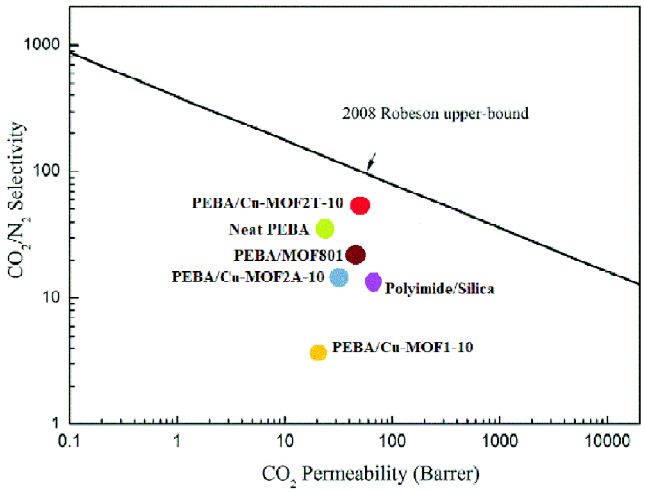

Fig. 11. Robeson plot for CO_2/N_2 and comparison of the PEBA/Cu-MOF2T-10, PEBA/Cu-MOF2A-10 and other MMMs.

Conclusions

Cu-MOFs was synthesized by two different synthesis methods. In the second synthesis method, two different modulators were used and two different nanocrystals were synthesized. PEBA/Cu-MOF MMMs were prepared with three different Cu-MOFs (10 wt%). Gas permeabilities of all MMMs at 3 bar pressure and 35°C was measured. After measuring the gas permeability, the selectivity of all MMMs was calculated. Cu-MOF-T-10 MMM gave the best permeability value.

The permeability value is 50.77 Barrer and the α_{CO_2/N_2} selectivity value is 51.80. These values were found to be higher than the studies in the literature.

References

1. P. Bernardo, E. Drioli and G. Golemme, *Ind. Eng. Chem. Res*., 2009, **48**, 4638.
2. Xu, H. Wu, Z. Wang, Z. Qiao, S. Zhao and J. Wang, *Chinese Journal of Chemical Engineering*, 2008, **26(11)**, 2280.
3. Sun, Q. Li, G. Chen, J. Duan, G. Liu W. Jin, *Sep. Purif. Technol.*, 2009, **217**, 229.
4. K. Keizer, R. J. Uhlhorn and T. Burggraaf, *Membrane Science and Technology*, Elsevier, 1995, Vol. 2, pp. 553-588.
5. S. Basu, A. Cano-Odena and I. Vankelecom, *Journal of Membrane Science*, 2010, **362(1-2)**, 478.
6. P. S. Goh, A. F. Ismail, S. M. Sanip, B. C. Ng and M. Aziz, *Sep. Purif. Technol.*, 2011, **81(3)**, 243.
7. R. Castro-Muñoz, F. Galiano, V. Fíla, E. Drioli and A. Figoli, *Reviews in Chemical Engineering*, 2019, **35(5)**, 565.
8. C. Dey, T. Kundu, B. P. Biswal, A. Mallick and R. Banerjee, *Acta Crystallographica Section B: Structural Science, Crystal Engineering and Materials,* 2014*,* **70(1)**, 3.
9. S. Carrasco, *Biosensors*, 2018, **8(4)**, 92.
10. Y. Yampolskii, *Macromolecules*, 2012, 453298.
11. L. Brinda, K. S. Rajan and J. B. B. Rayappan, *J. Appl. Sci.*, 2012, **12(16)**, 1778.
12. S. N. Nobar, *Materials Chemistry and Physics*, 2018, **213**, 343.
13. J. G. Wijmans and R. W. Baker, *Journal of Membrane Science*, 1995, **107(1-2)**, 1.
14. R. I. Masel, "Principles of Adsorption and Reaction on Solid Surfaces", John Wiley & Sons, 1996, Vol. 3.
15. H. Sanaeepur, R. Ahmadi, A. E. Amooghin and D. Ghanbari, *Journal of Membrane Science*, 2019, **573**, 234.
16. C. Hibshman, C. J. Cornelius and E. Marand, *Journal of Membrane Science*, 2003, **211(1)**, 25.
17. J. Sun, Q. Li, G. Chen, J. Duan, G. Liu and W. Jin, *Sep. Purif. Technol.*, 2019, **217**, 229.